

MULTICARRIER TECHNIQUES IN DIFFERENT WIRELESS ENVIRONMENTS

Igor Đurović, Đuro Stojanović¹

ABSTRACT:

The fast growth of the wireless data transmission requires reliable and high data-rate modulation techniques that can cope with impairments of the time-varying multipath channels. Multicarrier system based on the Fourier transform (FT), known as orthogonal frequency division multiplexing (OFDM), has been implemented in many practical multipath channels. The advantages of OFDM include robustness against multipath fading and high spectral efficiency. Nevertheless, it is highly sensitive to the time variation caused by the mobility. Typical environments that are inherently connected with the mobility are aeronautical, satellite and underwater acoustic channels. In these channels implementation of OFDM is limited and complicated channel estimation and interference cancellation is needed. However, leaving the FT concept and implementing different transformational basis opens new perspective in interference cancellation. In this paper, we investigated effects of time-varying multipath channels and present state-of-art in interference analysis of multicarrier systems based on the transforms that differ from FT. Namely, multicarrier system based on the affine Fourier transform (AFT-MC) significantly improves the interference suppression in channels with LOS component and narrow beamwidth of scattered components, which is a typical scenario in aeronautical and satellite channels. Similarly, multicarrier modulation based on the Mellin transform (MT-MC) efficiently cancels interference caused by Doppler scaling in wideband wireless channels such as underwater acoustic channels.

1 Introduction

The wireless channel is characterized by multipath propagation and time-varying fading. Multipath propagation occurs when signal propagates along different paths and multipath components arrive at the receiver at different times. Time-varying fading occurs due to the motion of the scatterers, transmitter or receiver. Transmission over the time-varying multipath

¹ Igor Đurović, Faculty of Electrical Engineering, University of Montenegro
Đuro Stojanović, Telekom Crne Gore, Podgorica

channels can lead to the *intersymbol interference* (ISI) caused by the time dispersion due to the multipath propagation, as well as the *interchannel interference* (ICI) caused by the time-variation [1]. Effects of mobility on transmitted signals are modeled differently for narrowband and wideband systems. In narrowband multipath environment, mobility causes frequency domain spreading (Doppler spreading), instead of time domain scale spreading (Doppler scaling) typical for the wideband channels.

Various multicarrier modulations with equally spaced subcarriers and overlapping spectra has been recently proposed for transmission in time-varying multipath channels. The orthogonal frequency division multiplexing (OFDM), based on the Fourier transform (FT), is one of the most important classes of multicarrier modulations [2]. It has been implemented in physical layer of many standardized wireless systems, such as digital audio broadcasting (DAB) [3], digital terrestrial TV broadcasting (DVB) [4], asymmetric digital subscriber line (ADSL) for high-bit-rate digital subscriber services [5], and wireless networks (IEEE 802.11a [6], IEEE 802.11g [7], IEEE 802.16-2004 [8] and HiperLAN/2 [9]).

The time variation due to mobility, coupled with dispersive scattering due to multipath propagation, induces interference that can severely derogate performance of the multicarrier systems. The OFDM symbol is typically preceded by a guard interval (in form of cyclic prefix or using zero padding) whose duration is longer than the delay spread of the propagation channel, that completely cancels ISI. However, OFDM is highly sensitive to ICI, due to time-variation caused by the mobility that destroys orthogonality between subcarriers [10]. Introduction of multicarrier techniques that differ from Fourier basis offers new ways for suppression of interference caused by the mobility.

Multicarrier techniques that are not based on the classical FT have been recently proposed by authors for transmission in channels where severe Doppler effects occur [11], [12]. In aeronautical and satellite channels, high velocity is an inherent part of the channel that system has to cope with. Multicarrier techniques based on the affine Fourier transform (AFT) are especially suitable for transmission in time-varying multipath channels with line-of-sight component and narrow beamwidth of scattered components that often occurs in aeronautical and satellite communications.

In a narrowband system, all subcarriers suffer from approximately same Doppler shift, and it is usual in interference analysis to use this narrowband assumption. This is not the case in wideband channels, where subcarriers suffer from different Doppler shifts. The OFDM systems has been also proposed for transmission in the wideband channels such as underwater acoustic channel [13]. However, a Doppler scaling of the channel induce

severe interference in the system. Considering the scaling nature of the wideband channel, a new multicarrier system based on the Mellin transform (MT-MC) has been recently proposed by the authors.

In this paper we investigate different multicarrier schemes in practical wireless channels and present implementation of new multicarrier techniques in aeronautical, satellite and underwater acoustic communications that authors have recently proposed in [10], [11] and [12]. Upper bounds on interference, as well as interference powers and interference power approximations have been presented in different wireless environments.

The paper is organized as follows. Section 2 provides narrowband channel characterization, followed by the wideband channel characterization in Section 3. Section 4 presents interference analysis of different multicarrier systems with practical examples. In Section 5 similar interference analysis in wideband system is provided. Finally, conclusions are given in Section 6.

2 Narrowband channel characterization

The multipath effects are quantified by *delay spread* τ_m and *coherence bandwidth* B_c . Multipath propagation causes variations of the channel over frequency that are characterized in terms of coherence bandwidth. The coherence bandwidth is frequency range over which channel characteristics remain correlated, and it is reciprocal of the delay spread. Delay spread causes effects of *time dispersion* and *frequency-selective fading*.

Time-varying fading occurs due to the motion of the scatterers, transmitter or receiver. The time-varying nature of the channel caused by movement is quantified by *Doppler spread* ν_m and *coherence time* T_c . Doppler spread ν_m describes effects of time-varying nature of the channel, whereas the coherence time, defined as an inverse of the Doppler spread, represents the time difference over which the channel response remains strongly correlated. Doppler spread causes effects of *frequency dispersion* and *time-selective fading*.

The coherence bandwidth and coherence time describe how the channel behaves for the transmitted signal. If B_c is smaller than the signal bandwidth B_s , the signal will exhibit frequency-selective fading. The correlation among different signal frequency components of the transmitted signal decreases toward zero. Received symbol duration becomes larger than the transmitted symbol duration and ISI occurs. For the channels where $B_s \ll B_c$, a signal is not subject to frequency-selective fading, and the channel is called *frequency-flat*. A time-selective fading channel occurs when T_c is shorter than the symbol duration T . Within a symbol duration channel appreciable

change its features. If $T_s \ll T_c$, a signal is not subject to time-selective fading, and the channel is called *time-flat*.

Wide-sense stationary uncorrelated scattering (WSSUS) model has been accepted as a standard stochastic model for the numerous wireless channels [14]. This model assumes that different delays and Doppler shifts are uncorrelated and that the correlation properties of the channel are stationary. This correlation properties can be expressed as

$$E [h(\tau, \nu)h^*(\tau_1, \nu_1)] = S(\tau, \nu)\delta(\tau - \tau_1)\delta(\nu - \nu_1), \quad (1)$$

where $h(\tau, \nu)$ represents delay-Doppler spread function and $S(\tau, \nu)$ denotes scattering function that completely characterizes the WSSUS model [14]. Scattering function provides description of the channel properties with respect to the delay variable τ and the frequency-domain variable ν (Doppler frequency). Projections of the scattering function along τ and ν are called the power delay profile $Q(\tau)$ (PDP) and Doppler power profile $P(\nu)$ (DDP) [15]

$$Q(\tau) = \int_{-\infty}^{\infty} S(\tau, \nu)d\nu, \quad (2)$$

$$P(\nu) = \int_{-\infty}^{\infty} S(\tau, \nu)d\tau, \quad (3)$$

respectively. Without loss of generality, scattering function can be assumed to be zero mean with total unit power $\int_{-\infty}^{\infty} \int_{-\infty}^{\infty} S(\tau, \nu)d\tau d\nu = 1$.

2.1 Multipath channels

Multipath channels can be divided into two categories: line-of-sight (LOS) multipath channels and non-line-of-sight (NLOS) multipath channels. Multipath scenario with LOS is generally referred as Rician fading, whereas NLOS multipath scenario is generally referred as Raleigh fading. Two main categories of LOS multipath channels can be defined: multipath channels with inseparable scattering function and multipath channels with separable scattering function. Furthermore, two special case of multipath scenario with separable scattering function are often used: two-ray multipath channel and single scatterer channel.

2.1.1 LOS multipath channels

The power of LOS σ_{LOS}^2 and the power of diffused components σ_{diff}^2 , for unchanged mean throughput power, can be defined as a function of the

Rician factor $K = \sigma_{LOS}^2 / \sigma_{diff}^2$ as

$$\sigma_{LOS}^2 = \frac{K}{K+1}, \quad (4)$$

$$\sigma_{diff}^2 = \frac{1}{K+1}. \quad (5)$$

The scattering function can be defined as

$$S(\tau, \nu) = \frac{K}{K+1} \delta(\tau) \delta(\nu - \nu_{LOS}) + \frac{1}{K+1} S_{diff}(\tau, \nu), \quad (6)$$

where $S_{diff}(\tau, \nu)$ denotes scattering function of multipath without LOS component.

Now, assume that $S_{diff}(\tau, \nu)$ is separable, i.e., $S_{diff}(\tau, \nu) = Q_{diff}(\tau)P_{diff}(\nu)$ and $\int_{-\nu_d}^{\nu_d} P_{diff}(\nu) d\nu = 1$, and $\int_0^{\tau_{diff}} Q_{diff}(\tau) d\tau = 1$, where τ_{diff} , $P_{diff}(\nu)$ and $Q_{diff}(\tau)$ denote maximum time delay, DPP and PDP of the scattered components, respectively. Here, the scattering function can be defined as

$$S(\tau, \nu) = \frac{K}{K+1} \delta(\tau) \delta(\nu - \nu_{LOS}) + \frac{1}{K+1} Q_{diff}(\tau) P_{diff}(\nu). \quad (7)$$

In the two-ray multipath channel, the scattering function takes form

$$S(\tau, \nu) = \frac{K}{K+1} \delta(\tau) \delta(\nu - \nu_{LOS}) + \frac{1}{K+1} P_{diff}(\nu) \delta(\tau - \tau_{diff}). \quad (8)$$

For the single scatterer case, channel model can be even further simplified. The scattering function has nonzero values only in two points $(0, \nu_{LOS})$ and $(\tau_{diff}, \nu_{diff})$

$$S(\tau, \nu) = \frac{K}{K+1} \delta(\tau) \delta(\nu - \nu_{LOS}) + \frac{1}{K+1} \delta(\tau - \tau_{diff}) \delta(\nu - \nu_{diff}). \quad (9)$$

2.1.2 NLOS multipath channel

NLOS channel follows from LOS for $K = 0$. In this case, $\sigma_{LOS}^2 = 0$, $\sigma_{diff}^2 = 1$, and all derived models can be directly implemented for the NLOS. However, it is commonly accepted that $S(\tau, \nu)$ is separable in the typical NLOS mobile channels [15].

2.2 Practical wireless channels

2.2.1 Land mobile wireless channel

Numerous radio propagation models for different wireless channels have been developed. COST 207 model is rather simple and widely used in research community [16]. It represents a comprehensive set of propagation scenarios that include NLOS and LOS cases with different delay and Doppler power profiles. Although these channel profiles were initially developed for GSM digital land mobile radio communications, they have also been used in other practical implementations (e.g. the COST 207 channel models is used as a non-directional realization of the COST 259 model [17]). The COST 207 defines four different environments: Rural Area (RA), Typical Urban (TU), Bad Urban (BU), and Hilly Terrain (HT). Power delay profile for the RA and TU can be described by exponential model as [18]

$$Q_{RA}(\tau) = \begin{cases} c_{\tau}e^{-9.2\tau/\mu s}, & \text{if } 0 \leq \tau < 0.7 \mu s, \\ 0, & \text{elsewhere,} \end{cases} \quad (10)$$

$$Q_{TU}(\tau) = \begin{cases} c_{\tau}e^{-\tau/\mu s}, & \text{if } 0 \leq \tau < 7 \mu s, \\ 0, & \text{elsewhere,} \end{cases} \quad (11)$$

respectively, where c_{τ} represents normalization factor. Power delay profile for the BU and HT can be represented by bimodal exponential model as [18]

$$Q_{BU}(\tau) = \begin{cases} c_{\tau}e^{-\tau/\mu s}, & \text{if } 0 \leq \tau < 5 \mu s, \\ 0.5c_{\tau}e^{5-\tau/\mu s}, & \text{if } 5 \mu s \leq \tau < 10 \mu s, \\ 0, & \text{elsewhere,} \end{cases} \quad (12)$$

$$Q_{HT}(\tau) = \begin{cases} c_{\tau}e^{-3.5\tau/\mu s}, & \text{if } 0 \leq \tau < 2 \mu s, \\ 0.1c_{\tau}e^{15-\tau/\mu s}, & \text{if } 15 \mu s \leq \tau < 20 \mu s, \\ 0, & \text{elsewhere,} \end{cases} \quad (13)$$

respectively.

For each of these propagation scenarios different types of Doppler power profile are also specified. The classical Jakes Doppler power profile occurs for very short propagation delays ($0 \leq \tau < 0.5 \mu\text{s}$) [18]

$$P(\nu) = \begin{cases} \frac{1}{\pi\nu_d} \frac{1}{\sqrt{1 - \left(\frac{\nu}{\nu_d}\right)^2}}, & \text{if } |\nu| < \nu_d, \\ 0, & \text{elsewhere.} \end{cases} \quad (14)$$

Distribution of scattered components with medium delays ($0.5 \mu\text{s} \leq \tau < 2 \mu\text{s}$) can be characterized by bimodal Gaussian Doppler power profile as [18]

$$P_{GAUSS1}(\nu) = c_\nu e^{-\frac{(\nu+0.8\nu_d)^2}{2(0.05\nu_d)^2}} + 0.1c_\nu e^{-\frac{(\nu-0.4\nu_d)^2}{2(0.1\nu_d)^2}}. \quad (15)$$

Similar Gaussian Doppler power profile characterizes scattered components with long delays ($\tau \geq 2 \mu\text{s}$) [18]

$$P_{GAUSS2}(\nu) = c_\nu e^{-\frac{(\nu-0.7\nu_d)^2}{2(0.1\nu_d)^2}} + 0.032c_\nu e^{-\frac{(\nu+0.4\nu_d)^2}{2(0.15\nu_d)^2}}. \quad (16)$$

It has been considered that the TU, BU and HT are NLOS models with Rayleigh fading. However, in the RA model LOS component occurs at $\tau = 0$, leading to the Rician fading. The scattering function consists of NLOS and LOS components and can be expressed as [18]

$$S_{RICE}(\tau, \nu) = c_\nu \frac{0.205}{\pi\nu_d \sqrt{1 - \left(\frac{\nu}{\nu_d}\right)^2}} Q(\tau) + 0.91c_\nu \delta(\nu - 0.7\nu_d) \delta(\tau), \quad (17)$$

where $c_\nu = 0.8969$. Now, signal power in LOS and NLOS part can be calculated as $\sigma_{LOS}^2 = 0.8161$, and $\sigma_{NLOS}^2 = 0.1839$. For the TU, BU and HT, $\sigma_{LOS}^2 = 0$, and $\sigma_{NLOS}^2 = 1$.

2.2.2 Aeronautical Channels

In aeronautical channel four different channel scenarios can be defined: en-route scenario, arrival and takeoff scenario, taxi scenario, and parking scenario [19]. In the en-route scenario, arrival and takeoff scenario and taxi scenario, a strong LOS component exists, whereas in the parking scenario there are only multipath components.

En-route scenario

The en-route scenario is model for ground-to-air or air-to-air communications when the aircraft is airborne. For this multipath channel, a two-ray model with a LOS path and cluster of scattered paths is used. Typical maximal velocities are $v_{\max} = 440$ m/s for ground-air links and $v_{\max} = 620$ m/s for air-air links. In this scenario the scattered components are not uniformly distributed in the interval $[0, 2\pi)$ leading to the asymmetrical DPP. Actually, the beamwidth of the scattered components is reported to be around 3.5° . In this case, $S(\tau, \nu)$ takes form (8) where $P_{diff}(\nu)$ can be modeled by restricted Jakes model [20]

$$P_{diff}(\nu) = \psi \frac{1}{\nu_d \sqrt{1 - \left(\frac{\nu}{\nu_d}\right)^2}}, \nu_1 \leq \nu \leq \nu_2, \quad (18)$$

where $\psi = 1/(\arcsin(\nu_2/\nu_d) - \arcsin(\nu_1/\nu_d))$, denotes factor introduced to normalize DPP.

In the worst case the LOS component comes directly to the front of the aircraft and scattered components come from behind. Here, $\nu_1 = -\nu_d$ and $\nu_2 = -\nu_d(1 - \Delta\varphi_B/\pi)$, where $\Delta\varphi_B$ represents the beamwidth of the scattered components symmetrically distributed around the $\varphi = \pi$.

Arrival and Takeoff Scenario

The arrival and takeoff scenario models communications between ground and aircraft when the aircraft takeoffs or is about to land. It is assumed that the LOS and scattered components arrive directly in front of the aircraft and the beamwidth of the scattered components from the obstacles in the airport is 180° . The maximal speed of the aircraft is 150 m/s, and the Rician factor $K = 15$ dB. In this channel, $S(\tau, \nu)$ is separable and takes form (8) where $P_{diff}(\nu)$ can be modeled by Jakes model (18), with $\nu_1 = 0$ and $\nu_2 = \nu_d$. The PDP can be modeled as an exponential function similarly to the rural nonhilly COST 207 model.

Taxi Scenario

The taxi scenario is model for communications when the aircraft is on the ground and approaching or moving away from the terminal. The LOS path comes from the front, but not directly, resulting in smaller Doppler shifts, for example $\nu_{LOS} = 0.7\nu_d$. The maximal speed is 15 m/s, and the reflected paths come uniformly, resulting in classical Jakes DPP (18), with $\nu_1 = -\nu_d$ and $\nu_2 = \nu_d$. The PDP can be modeled similarly to the rural (nonhilly) COST 207 model.

Parking Scenario

The parking scenario models the arrival of the aircraft to the terminal or parking. The LOS path is blocked, resulting in Rayleigh fading. The maximal speed of the aircraft is 5.5 m/s, and DPP can be modeled as a classical

Jakes profile (18) with $\nu_1 = -\nu_d$ and $\nu_2 = \nu_d$. The parking scenario is similar to the typical urban COST 207 model.

2.2.3 Land-Mobile Satellite Channels

Land-mobile satellite (LMS) communications represents another example of channels with strong LOS component and scattered multipath components. In Land-Mobile Low Earth Orbit (LEO) satellite channel, mobile terminal uses a narrow-beam antenna (e.g. digital beamforming antenna - DBF) to track and communicate with LEO satellite [21]. If we assume that mobile terminal is out of urban areas, the PDP can be modeled as an exponential function similarly to the rural nonhilly COST 207 model and DPP can be modeled by restricted Jakes model (18). The arrival angles of the multipath components are uniformly distributed, but antenna is narrow-beam leading to the equivalent scenario in that occurs in aeronautical channel when antenna is omnidirectional but multipath components comes from narrow angle. Now, previous analysis for en-route scenario in aeronautical channel can be directly implemented in LMS channel analysis.

3 Wideband channel characterization

When a signal has a small time-bandwidth product or when the relative motion is slow, Doppler scalings can be approximated by fixed frequency shifts [22]. Physical interpretation of the system output can be made in terms of time and frequency shifts on the input signal. This interpretation is applied to describe the time-varying multipath environment of narrowband communication channels. The physical effects of the wideband system on the signal are characterized by time shifts τ and Doppler scalings a . Just as the time-frequency model characterizes narrowband processing, a time-scale model describes wideband time-varying systems [23].

The typical wideband system can be described by wide-sense stationary uncorrelated scattering (WSSUS) model. If the system is WSSUS, then different delays and Doppler scalings are uncorrelated and the correlation properties of the channel are stationary. These correlation properties can be expressed by wideband scattering function $\Omega(\tau, a)$ that quantifies the distribution of received power as a function of delay and scale [23]

$$E \{ \chi(\tau, a) \chi^*(\tau', a') \} = \Omega(\tau, a) \delta(a - a') \delta(\tau - \tau'), \quad (19)$$

where $\chi(\tau, a)$ represents wideband spreading function. Wideband scattering function $\Omega(\tau, a)$ provides description of the channel properties with respect

to the delay variable τ and the scale variable a . Define projections of the wideband scattering function along τ and a as power delay profile $Q(\tau)$ and scale power profile $P(a)$

$$Q(\tau) = \int_{a_{\min}}^{a_{\max}} \Omega(\tau, a) da, \quad (20)$$

$$P(a) = \int_0^{\tau_{\max}} \Omega(\tau, a) d\tau, \quad (21)$$

respectively. Power delay profile is well-known from narrowband channels and models that characterize narrowband case can be directly used (e.g. uniform and exponential models [20]). Let us now analyze distribution of received power as a function of the scale variable a . In wideband channels scale power profile $P(a)$ corresponds to the Doppler power profile from the narrowband channels. The scale variable a can be expressed as [24]

$$a = 1 - \frac{v}{c} \cos(\varphi), \quad (22)$$

where v represents velocity, c denotes speed of wave propagation and φ represents arriving angle of path in radians. The minimum and the maximum scale are defined as $a_{\min} = 1 - v_{\max}/c$ and $a_{\max} = 1 + v_{\max}/c$, respectively. A scale spread, that corresponds to the Doppler spread in narrowband channels, defined as $\gamma_{\max} = \frac{1}{2}(a_{\max} - a_{\min})$ can be expressed as [24]

$$\gamma_{\max} = \frac{v_{\max}}{c}. \quad (23)$$

The scale power profile characterizes time-variation of wideband channels, and it can be modeled as a counterpart of the Doppler power profile, that defines Doppler spreading in narrowband channels. Similarly to the Doppler power profile [20], scale power profile $P(a)$ can be modeled as two-path, uniform, and classical (Jakes).

Two-path Doppler power profile model is often used in narrowband channels when there are direct and reflected path. A corresponding scale power profile can be expressed as [12]

$$P(a) = \frac{1}{2} [\delta(1 - a + \gamma_{\max}) + \delta(1 - a - \gamma_{\max})]. \quad (24)$$

Uniform Doppler power profile model is another simple representation. It describes 3-D isotropic scattering environment, where the angles of arrival

are uniformly distributed in the azimuth and elevation planes. The scale power profile in this case can be expressed as [12]

$$P(a) = \begin{cases} \frac{1}{2\gamma_{\max}}, & \text{if } 1 - \gamma_{\max} < a < 1 + \gamma_{\max}, \\ 0, & \text{elsewhere.} \end{cases} \quad (25)$$

In case of horizontal propagation of radio waves, uniformly distributed angles of arrival and omnidirectional antenna, the Doppler power profile is called classical or Jakes. The corresponding scale power profile can be modeled as [12]

$$P(a) = \begin{cases} \frac{1}{\pi\gamma_{\max}} \frac{1}{\sqrt{1 - \left(\frac{1-a}{\gamma_{\max}}\right)^2}}, & \text{if } 1 - \gamma_{\max} < a < 1 + \gamma_{\max}, \\ 0 & \text{elsewhere.} \end{cases} \quad (26)$$

4 Interference Power Analysis in Narrowband Channels

Let us now consider the baseband of the multicarrier signal

$$s(t) = \sum_{n=-\infty}^{\infty} \sum_{k=0}^{K-1} c_{n,k} g_{n,k}(t), \quad (27)$$

where $c_{n,k}$ denotes the data symbol and $g_{n,k}(t)$ denotes the translation and modulation of a normalized single pulse shape $g(t)$, where n and k correspond to the symbol interval and the subcarrier number at the transmitter. In analogy with the classical ambiguity function definition $A(\tau, \nu) = \int_{-\infty}^{\infty} g(t)g^*(t - \tau)e^{-j2\pi\nu t} dt$, the linearly transformed ambiguity function $A(\tau_p, \nu_p)$ can be defined as

$$A(\tau_p, \nu_p) = \int_{-\infty}^{\infty} g(t)g^*(t - \tau_p)e^{-j2\pi\nu_p t} dt. \quad (28)$$

Under the assumption of wide sense stationary uncorrelated scattering (WS-SUS) channel [14], average useful power can be expressed as [25]

$$P_U = \int_{-\infty}^{\infty} \int_{-\infty}^{\infty} S(\tau, \nu) |A(\tau, \nu)|^2 d\tau d\nu. \quad (29)$$

The interference power can be obtained as [25]

$$P_I = \int_{-\infty}^{\infty} \int_{-\infty}^{\infty} S(\tau, \nu) \sum_{(n,k) \neq (n',k')} |A(\tau_p, \nu_p)|^2 d\tau d\nu. \quad (30)$$

4.1 OFDM

The translations and modulations by the OFDM pulse shape $g(t)$ can be represented as

$$g_{n,k}(t) = g(t - nT)e^{j2\pi kF(t-nT)}, \quad (31)$$

where $F = 1/T$ represents carrier spacing. The linearly transformed ambiguity function $A(\tau_p, \nu_p)$ for OFDM can be obtained for

$$\begin{aligned} \tau_p &= (n' - n)T + \tau, \\ \nu_p &= (k' - k)F + \nu. \end{aligned} \quad (32)$$

where n' and k' correspond to the symbol interval and the subcarrier number at the receiver. Interference power can be simplified for the case of rectangular pulses as [10]

$$P_I = 1 - \int_{-\nu_d}^{\nu_d} \int_0^{\tau_{\max}} S(\tau, \nu) \text{sinc}^2(\pi T \nu) d\tau d\nu. \quad (33)$$

An upper bound on interference power when the guard interval is not implemented, can be expressed as [10]

$$\begin{aligned} P_{IUB} &= \frac{1}{3}\gamma_{2,0}\pi^2\nu_d^2T^2 + 2\gamma_{0,1}\frac{\tau_{\max}}{T} - \gamma_{0,2}\frac{\tau_{\max}^2}{T^2} \\ &\quad - \frac{4}{3}\gamma_{2,1}\pi^2\nu_d^2T\tau_{\max} + 2\gamma_{2,2}\pi^2\nu_d^2\tau_{\max}^2 \\ &\quad - \frac{4}{3}\gamma_{2,3}\pi^2\nu_d^2\frac{\tau_{\max}^3}{T} + \frac{1}{3}\gamma_{2,4}\pi^2\nu_d^2\frac{\tau_{\max}^4}{T^2}. \end{aligned} \quad (34)$$

where parameters γ_{ij} for $i, j \in N$ characterize impact of the power profiles on the system

$$\gamma_{i,j} = \frac{1}{\nu_d^i} \frac{1}{\tau_{\max}^j} \int_{-\nu_d}^{\nu_d} \int_{t_1}^{t_2} S(\tau, \nu) \nu^i \tau^j d\tau d\nu.$$

Now, an approximate interference power for OFDM can be obtained as [10]

$$P_I \cong P_{ICI} + P_{ISI}, \quad (35)$$

where P_{ICI} and P_{ISI} are

$$P_{ICI} = \frac{1}{3}\gamma_{2,0}\pi^2\nu_d^2T^2, \quad (36)$$

$$P_{ISI} = 2\gamma_{0,1}\frac{\tau_{\max}}{T} - \gamma_{0,2}\left(\frac{\tau_{\max}}{T}\right)^2. \quad (37)$$

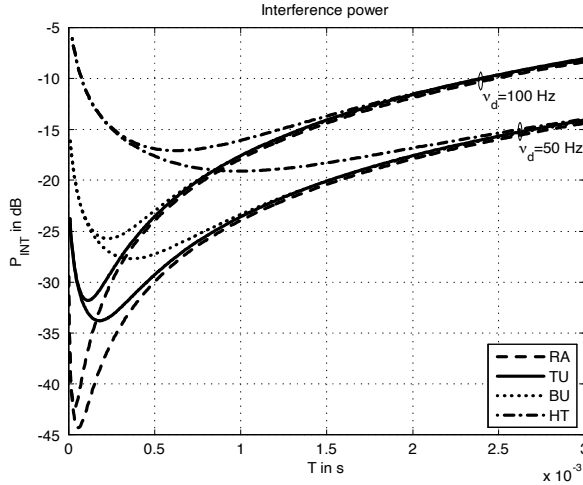


Figure 1: Interference power when cyclic prefix covers 75% of maximal delay in COST 207 channel models (Rural Area - RA, Typical Urban - TU, Bad Urban - BU, and Hilly Terrain - HT).

If the guard interval is implemented, the interference power can be easily obtained from the previous equations by equaling $\gamma_{ij} = 0$ for $i \neq 0$.

In Fig. 1 we compare interference power in the COST 207 RA, TU, BU and HT channel models, with cyclic prefix covers 75% of maximal delay, $\nu_d = 50$ Hz and 100 Hz. We can observe from Figs. 1 that when T increases interference power converges towards P_{ICI} , whereas, when T or GI decreases, interference power converges towards P_{ISI} .

4.2 AFT-MC

The translations and modulations by a chirp basis of a single normalized pulse shape $g(t)$ can be written as

$$g_{n,k}(t) = g(t - nT)e^{j2\pi(c_1^2(t-nT)^2 + c_2k^2 + \frac{k}{T}(t-nT))}, \quad (38)$$

where T is the symbol period, and c_1 and c_2 are the AFT parameters. Usually, frequency offset correction block, that can be modeled as $e^{j2\pi c_0 t}$, is inserted in the receiver. The linearly transformed ambiguity function

$A(\tau_p, \nu_p)$ for AFT-MC can be obtained for

$$\begin{aligned}\tau_p &= (n' - n)T + \tau, \\ \nu_p &= \frac{1}{T} (k' - k) + \nu - c_0 - 2c_1((n' - n)T + \tau).\end{aligned}\quad (39)$$

In case of rectangular pulses as the interference power can be expressed as [11]

$$P_I = 1 - \int_{-\nu_d}^{\nu_d} \int_0^{\tau_{\max}} S(\tau, \nu) \text{sinc}^2 \pi T (\nu - c_0 - 2c_1 \tau) d\tau d\nu. \quad (40)$$

The AFT-MC system reduces respectively to the fractional FT (FrFT) and OFDM based system for $c_1 = \cot \alpha / (4\pi)$ and $c_1 = 0$. The upper bound on interference power with the guard interval implemented, can be expressed as [11]

$$P_{IUB} = \frac{1}{3} m_{20}(c_0, c_1) \pi^2 T^2, \quad (41)$$

where $m_{ij}(c_0, c_1)$ for $i, j \in N$ represent moments of the scattering function for AFT-MC

$$\begin{aligned}m_{ij}(c_0, c_1) &= \int_{-\nu_d}^{\nu_d} \int_0^{\tau_{\max}} S(\tau, \nu) \\ &\quad \times (\nu - c_0 - 2c_1 \tau)^i \tau^j d\tau d\nu.\end{aligned}\quad (42)$$

An approximate interference power for the wide range of channel parameters can be obtained as [11]

$$P_I \cong \frac{\frac{1}{3} \sigma_{diff}^2 m_{20}(c_0, c_1) \pi^2 T^2}{\sigma_{diff}^2 + \frac{1}{3} m_{20}(c_0, c_1) \pi^2 T^2}. \quad (43)$$

Fig. 2 compares OFDM and AFT-MC interference power in en-route scenario in aeronautical channel. Parameters for this scenario are: carrier frequency $f_c = 1.55\text{GHz}$ (corresponding to the L band), $\Delta\varphi_B = 3.5^\circ$, $\tau_{diff} = 66\mu\text{s}$, $T = 1056\mu\text{s}$ and $K = 15\text{dB}$. Maximal Doppler shift depends on the velocity of the aircraft $\nu_d = v_{\max} f_c / c$, where c denotes speed of light and maximal velocity is assumed to be up to $v_{\max} = 250\text{ m/s}$. From Fig. 2, it can be observed that the AFT-MC system efficiently suppresses interference even for the large Doppler shifts. The approximated interference powers stay close to the exact ones (in AFT-MC case, they are practically indistinguishable). When GI is implemented, the interference power in the AFT-MC is negligible, comparing to its significant value in the OFDM. Similar to the en-route scenario in aeronautical communications, this type of channel also occurs in various satellite communications (e.g. in LMS).

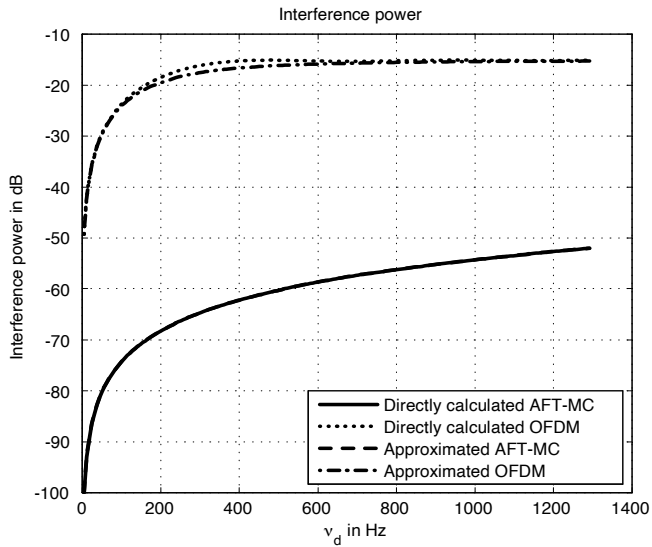


Figure 2: Comparison of directly calculated and approximated interference power in the en-route scenario in aeronautical channels for AFT-MC and OFDM.

5 Interference Power Analysis in Wideband Channels

Consider the multicarrier signal

$$s(t) = \sum_{k=0}^{M-1} c_k g_k(t). \quad (44)$$

The average useful power on the k subcarrier can be expressed as [12]

$$P_D^{(k)} = \int_{a_{\min}}^{a_{\max}} \int_0^{\tau_{\max}} \Omega(\tau, a) |\Theta(\tau, a)|^2 d\tau da, \quad (45)$$

where $\Theta(\tau, a)$ represents system characteristics that depends on the pulse shape. The interference power can be obtained by [12]

$$P_I^{(k)} = \int_{a_{\min}}^{a_{\max}} \int_0^{\tau_{\max}} \Omega(\tau, a) \sum_{k \neq k'} |\Theta(\tau, a)|^2 d\tau da. \quad (46)$$

Consider $\Theta(\tau, a)$ and $\Omega(\tau, a)$ are given with unit power, and assume that there is an infinite number of subcarriers. The interference power can be expressed as [12]

$$P_I^{(k)} = 1 - \int_{a_{\min}}^{a_{\max}} \int_0^{\tau_{\max}} \Omega(\tau, a) |\Theta(\tau, a)|^2 d\tau da. \quad (47)$$

5.1 OFDM

Consider the wideband representation of the transmitter and receiver OFDM modulated pulses $g_{k'}(a(t - \tau))$ and $g_k(t)$ at the receiver

$$g_{k'}(a(t - \tau)) = g(a(t - \tau)) e^{j2\pi(\frac{k'}{T} + f_0)a(t - \tau)}, \quad (48)$$

$$g_k(t) = g(t) e^{j2\pi(\frac{k}{T} + f_0)t}, \quad (49)$$

respectively, where $\frac{k}{T}$ and f_0 denote carrier spacing and the first subcarrier frequency.

The interference power $P_I^{(k)}$ can be expressed as [12]

$$P_I^{(k)} = \int_{a_{\min}}^{a_{\max}} P(a) \sum_{k \neq k'} \text{sinc}^2 \pi(k - k'a + f_0 T(1 - a)) da. \quad (50)$$

The interference power $P_I^{(k)}$ can be obtained by [12]

$$P_I^{(k)} = 1 - \int_{a_{\min}}^{a_{\max}} P(a) \times \text{sinc}^2 \pi(k + f_0 T)(1 - a) da. \quad (51)$$

An upper bound on intercarrier interference power with the guard interval implemented, can be derived by using Taylor series as [12]

$$P_{IUB}^{(k)} = \frac{1}{3} \alpha_2 \pi^2 (k + f_0 T)^2 \gamma_{\max}^2, \quad (52)$$

where α_2 equals

$$\alpha_2 = \frac{1}{\gamma_{\max}^2} \int_{a_{\min}}^{a_{\max}} P(a) (1 - a)^2 da. \quad (53)$$

Fig. 3 illustrates comparison of OFDM interference powers directly calculated by summation (50), using useful power (51), and upper bound (52). Parameters for this scenario are: $f_0 = 4\text{kHz}$, $T = 256\text{ ms}$, $M = 512$, and $\gamma_{\max} = 4 \cdot 10^{-5}$. Three different scale power profiles are used: two-path, uniform and classical, where corresponding α_2 equal to 1, 1/3, 1/2, respectively. We can observe from Fig. 3 that the interference power depends on the sub-carrier number and scale power profile. The difference between interference powers calculated by (50) and (51), and upper bound on interference power calculated by (52) is negligible, except for the subcarriers on the edge, where only directly calculated interference gives the exact result.

5.2 Mellin transform

The Mellin transform, unlike the FT, possesses the property of being scale-invariant in its magnitude [23]. This property offers an excellent opportunity for combating effects of Doppler scaling. Define the wideband representation of modulated transmitter and receiver pulses $g_{k'}(a(t - \tau))$ and $g_k(t)$ at the MT-MC receiver as

$$g_{k'}(a(t - \tau)) = g(a(t - \tau)) \frac{1}{\sqrt{a(t - \tau)}} \times e^{j2\pi(k'\beta + \beta_0) \ln \frac{a(t - \tau)}{t_r}}, \quad (54)$$

$$g_k(t) = g(t) \frac{1}{\sqrt{t}} e^{j2\pi(k\beta + \beta_0) \ln \frac{t}{t_r}}, \quad (55)$$

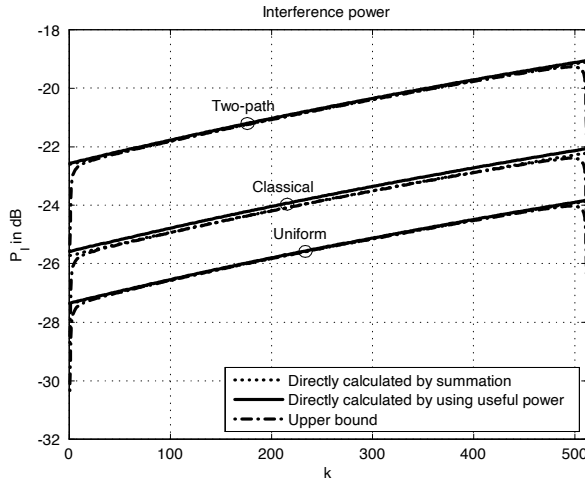


Figure 3: The comparison of OFDM interference power for different subcarriers k and scale power profiles (from top to bottom: two-path, classical, and uniform scale power profile).

respectively, where β and β_0 denote scaling spacing and scaling factor of the first subcarrier, and t_r represents normalization time point. $|\Theta(\tau, a)|^2$ can be obtained as [12]

$$\begin{aligned} |\Theta(\tau, a)|^2 &= \text{sinc}^2 \pi(k - k') \\ &= \begin{cases} 1, & \text{for } k' = k \\ 0, & \text{for } k' \neq k. \end{cases} \end{aligned} \quad (56)$$

Now, the desired power P_d for $k = k'$ equals $P_D = 1$, whereas the interference power P_I is equal to 0. Thus, orthogonality between subcarriers has been preserved. It follows that contrary to the OFDM, the MT-MC system completely suppresses interference in wideband time-varying multipath channels. Actually, this is a result of a scale invariance of the Mellin transform that is essential to efficient multicarrier transmission in wideband channel.

6 Conclusion

Conventional OFDM system has been initially proposed for communications in the narrowband channels where Doppler effects can be mitigated. How-

ever, in aeronautical, satellite and underwater acoustic channels Doppler effects severely degrade performances of OFDM. This impairments occur due to Fourier transform basis of OFDM that is not an adequate transform for the these channels. In this paper, we investigated effects of time-varying multipath channels and present state-of-art of interference analysis. The interference characteristics of narrowband and wideband channels are presented with comparison of OFDM, AFT-MC and MT-MC systems in different wireless environments. The AFT-MC systems clearly outperform OFDM in aeronautical and satellite channels whereas MT-MC systems completely neutralize effects of Doppler scaling in underwater acoustic channels and represent better choice than OFDM.

References

- [1] J. G. Proakis, *Digital Communications*, 4th. ed., New York: McGraw-Hill, 2000.
- [2] J. A. C. Bingham, "Multicarrier modulation for data transmission: an idea whose time has come," *IEEE Commun. Mag.*, vol. 28, no. 5, pp. 5-14, May 1990.
- [3] ETSI, "Radio Broadcasting Systems; Digital Audio Broadcasting (DAB) to Mobile, Portable and Fixed Receivers," European Telecommunications Standards Institute, ETS 300 401 2nd edition, Valbonne, France, 1997.
- [4] ETSI, "Digital Video Broadcasting (DVB); Framing Structure, Channel Coding and Modulation for Digital Terrestrial Television," European Telecommunications Standards Institute, ETS EN 300 744 v 1. 1. 2, 1997.
- [5] ANSI, "Network and Customer Installation Interfaces - Asymmetric Digital Subscriber Line (ADSL) Metallic Interface," ANSI standard T1, 1995.
- [6] IEEE 802. 11a, IEEE Standard for Information technology—Telecommunications and information exchange between systems—Local and metropolitan area networks—Specific requirements—Part 11: Wireless LAN Medium Access Control (MAC) and Physical Layer (PHY) specifications—Amendment 1: High-speed Physical Layer in the 5 GHz band, 1999.

-
- [7] IEEE 802. 11g, IEEE Standard for Information technology—Telecommunications and information exchange between systems—Local and metropolitan area networks—Specific requirements—Part 11: Wireless LAN Medium Access Control (MAC) and Physical Layer (PHY) specifications—Amendment 4: Further Higher-Speed Physical Layer Extension in the 2.4 GHz Band, 2003.
 - [8] IEEE Standard 802. 16-2004, IEEE Standard for Local and Metropolitan Area Networks - Part 16: Air Interface for Fixed Broadband Wireless Access Systems, 2004.
 - [9] ETSI, “Broadband Radio Access Networks (BRAN); High Performance Radio Local Area Network (HIPERLAN) Type 2; Requirements and Architectures for Wireless Broadband Access,” TR 101 031 (1999-01), v. 1. 1. 1, 1999.
 - [10] Dj. Stojanovic, B. R. Vojcic, and I. Djurovic, “Bounds on the Interference of OFDM in Time-Varying Multipath Channels,” *IEEE Trans. Wireless Comm.*, 2009, (submitted).
 - [11] Dj. Stojanovic, I. Djurovic, and B. R. Vojcic, “Interference Analysis of Multicarrier Systems based on Affine Fourier Transform,” *IEEE Trans. Wireless Comm.*, 2009, (accepted for publishing).
 - [12] Dj. Stojanovic, and I. Djurovic, “A Wideband Multicarrier System Based on the Mellin Transform in Underwater Acoustic Communications,” *IEEE SPAWC-09*, June 2009, (submitted).
 - [13] E. Bejjani, and J. C. Belfiore, “Multicarrier Coherent Communications for the Underwater Acoustic Channel,” in *Proc. of OCEANS*, 1996.
 - [14] P. A. Bello, “Characterization of randomly time-variant linear channels,” *IEEE Trans. Commun. Syst.*, vol. 11, no. 4, pp. 360-393, Dec. 1963.
 - [15] P. A. Bello, “Aeronautical Channel Characterization,” *IEEE Trans. Commun. Syst.*, vol. 21, no. 5, pp. 548-563, May 1973.
 - [16] M. Falli, Ed., *Digital land mobile radio communications - COST 207: Final report*, Luxembourg: Commission of European Communities, 1989.
 - [17] H. Asplund, A. A. Glazunov, A. F. Molisch, K. I. Pedersen, and M. Steinbauer, “The COST 259 Directional Channel Model - Part II: Macrocells,” *IEEE Trans. Wireless Comm.*, vol. 5, no 12, pp. 3434-3450, Dec. 2006.

-
- [18] M. Ibnkahla, Ed., *Signal Processing for Mobile Communications Handbook*, Boca Raton: CRC Press, 2004.
 - [19] E. Haas, "Aeronautical Channel Modeling," *IEEE Trans. Veh. Technol.*, vol. 51, no. 2, pp. 254–264, March 2002.
 - [20] M. Paetzold, *Mobile Fading Channels*, Wiley, New York, 2002.
 - [21] M. Rice and E. Perrins, "A Simple Figure of Merit for Evaluating Interleaver Depth for the Land-Mobile Satellite Channel," *IEEE Trans. Commun.*, vol. 49, no. 8, pp. 1343–1353, Aug. 2001.
 - [22] L. G. Weiss, "Wavelets and Wideband Correlation Processing," *IEEE Signal Process. Mag.*, vol. 11, no. 1, pp. 13–32, Jan. 1994.
 - [23] Y. Jiang and A. Papandreou-Suppappola, "Discrete Time-Scale Characterization of Wideband Time-Varying Systems," *IEEE Trans. Signal Process.*, vol. 54, no. 4, pp. 1364–1375, Apr. 2006.
 - [24] A. R. Margetts, P. Schniter, and A. Swami, "Joint Scale-Lag Diversity in Wideband Mobile Direct Sequence Spread Spectrum Systems," *IEEE Trans. Wireless Comm.*, vol. 6, no. 12, pp. 4308–4319, Dec. 2007.
 - [25] K. Liu, T. Kadous, and A. Sayeed, "Orthogonal Time-Frequency Signaling Over Doubly Dispersive Channels," *IEEE Trans. Info. Theory*, vol. 50, no. 11, pp. 2583–2603, Nov. 2004.

